Electronic Supporting Information (ESI)

Exploring a new short-wavelength nonlinear optical fluoride material featuring unprecedented polar *cis*-$[Zr_6F_{34}]^{10-}$ clusters

Mei Yan, [a] Ru-Ling Tang, [a]* Wen-Dong Yao, [a] Wenlong Liu, [a] and Sheng-Ping Guo [a]*

a School of Chemistry and Chemical Engineering, Yangzhou University, Yangzhou, Jiangsu 225002, P. R. China

Corresponding authors: rltang@yzu.edu.cn, spguo@yzu.edu.cn

CONTENTS

1. Experimental Section

2. Tables and Figures

Table S5. Summary of fluorides with 31 F elements in the formula.

Table S6. Summary of fluorine-rich fluorides (F > 30).

Table S7. The dipole moments of ZrF_8 units in the unit cell of $K_3Ba_2Zr_6F_{31}$.

Figure S1. (a) Powder X-ray diffraction pattern and (b) EDS image of $K_3Ba_2Zr_6F_{31}$.

Figure S2. (a) $[Zr(1)_3F_{19}]^{7-}$ clusters made up of edge-sharing $Zr(1)F_8$ units and (b) $[Zr(2)_3F_{21}]^{9-}$ clusters formed by vertex-sharing $Zr(2)F_8$ units.

Figure S3. Coordination modes of K(1) and Ba(1) atoms.

Figure S4. (a) TG curves and (b) XRD patterns of $K_3Ba_2Zr_6F_{31}$ samples heated at different temperatures.

Figure S5. (a) Calculated band structure and (b) density of states (DOS) of $K_3Ba_2Zr_6F_{31}$. The Fermi level is chosen at 0 eV.

Figure S6. Calculated refractive index dispersion curves and PM range of $K_3Ba_2Zr_6F_{31}$.

3. References

1. Experimental Section

Caution! Hydrofluoric acid is toxic and volatile. All of the experiments must be performed with extreme care and proper protection.

Synthesis

The following reagents were used as received in this work: KF (Macklin, 99 %), ZrF_4 (Adamas, AR), $BaCl_2{\cdot}2H_2O$ (Sinopharm Chemical Reagent, AR), and hydrofluoric acid (HF, Aladdin, 40%). $K_3Ba_2Zr_6F_{31}$ were prepared via hydrothermal reactions with stoichiometric ratio (KF : ZrF_4 : $BaCl_2{\cdot}2H_2O$ = 1.5 : 1 : 2), 3 ml deionized water and 1.5 ml HF solution were also added into the 20 ml Teflon-lined stainless-steel autoclaves. The autoclaves were heated from room temperature to 200 ℃ in 3 h, kept for 3 days, and finally cooled to 40 ℃ at a rate of 2.5 ℃/h. Colorless crystals of $K_3Ba_2Zr_6F_{31}$ can grow up to $5 \times 1 \times 1$ mm^3 with good habit of growth and satisfying yield of 70 % based on ZrF_4.

Single-crystal structure determination

Colorless and transparent single crystals of were selected for single-crystal X-ray diffraction (SXRD) collection, and the data was obtained on a Bruker D8 QUEST X-ray diffractometry (λ = 0.71073 Å) at 296 K. Concrete crystal structure was solved by direct method and refined by the SHELXTL program on Olex2 package.[1] The structure was then checked by ADDSYM algorithm from the program PLATON, and no missed or higher symmetries were proposed. The crystallographic data is listed in Table S1. The atomic coordinates, isotropic displacement coefficients, and bond valence sums are summarized in Table S2. Bond lengths are displayed in Table S3. CCDC number: 2305228.

Powder X-ray diffraction characterization

Experimental powder X-ray diffraction (PXRD) pattern was collected on a Bruker D8 Advance diffractometer equipped with Cu kα radiation at room temperature, with a step size of 0.02 ° in the range 2θ = 10–60 °. The simulated pattern was solved by Mercury program. The exact match between the two proves the purity of the polycrystalline powder samples of $K_3Ba_2Zr_6F_{31}$ (Figure S1a).

Element analysis

Element analysis was performed by an energy dispersive X-ray spectroscope (EDS, Bruker, Quantax) with an acceleration voltage of 20 kV for $K_3Ba_2Zr_6F_{31}$, and the result demonstrates the existence of K, Ba, Zr, and F elements (Figure S1b).

Thermal analysis

Under nitrogen flow, the thermogravimetric analysis (TGA) of $K_3Ba_2Zr_6F_{31}$ was performed with the a Netzsch STA449F3 simultaneous analyzer from 20 to 1000 °C at the rate of 10 °C/min (Figure S2).

Optical properties

UV-vis-NIR diffuse reflectance spectrum of $K_3Ba_2Zr_6F_{31}$ was collected on powder samples with $BaSO_4$ as standard on a Carry 5000 UV-vis-NIR spectrometer, and the spectral range is set as 200–1400 nm. IR spectrum was recorded in the range of 400 to 4000 cm^{-1} on a Fourier transform IR spectrometer.

SHG measurement

Powder SHG response was investigated by the Q-witched Nb: YAG laser (1064 nm) based on the Kurtz and Perry method.[2] The Polycrystalline sample were sieved to six particle size ranges, including 25–45, 45–75, 75–110, 110–150, 150–200, and 200–250 μm. The polycrystalline sample of KDP crystal was ground into the same size ranges and tested as reference.

Electronic structure calculations

Band structure and density of states (DOS) of $K_3Ba_2Zr_6F_{31}$ was calculated with the structural mode obtained from the SXRD analysis on the basis of the density functional theory (DFT) method with CASTEP mode.[3,4] The following orbital electrons were chosen as valence electrons, K $3s^23p^64s^1$, Ba $5s^25p^66s^2$, Zr $4s^24p^64d^25s^2$, and F $2s^22p^5$ electrons. The plane-wave basis energy cutoff was set as 850 eV, and the k-points with 3 × 3 × 2 was chosen in the first Brillouin zone. Heyd–Scuseria–Ernzerhof (HSE06) hybrid functional implemented was utilized for accurate bandgap of $K_3Ba_2Zr_6F_{31}$ due to the discontinuity of exchange-correlation energy and the underestimated calculated band gap.[5] The optical property was calculated by using the same method that can be referred to our previous works.[6] The polarizability anisotropies of ZrF_8, MgF_6, AlF_6, and ZnF_6 species in $K_3Ba_2Zr_6F_{31}$, $BaMgF_6$, $SrAlF_5$, and $BaZnF_6$ were calculated by the Gaussian 09 package at B3LYP/QZVPD level.[7]

Table S1. Crystal data and structure refinement parameters for $K_3Ba_2Zr_6F_{31}$.

Empirical formula	$K_3Ba_2Zr_6F_{31}$
Formula weight	1528.30
T/K	296(2)
Crystal system	hexagonal
Space group	$P6_3mc$
a/Å	9.4435(3)
c/Å	15.3288(6)
Volume/Å^3	1183.87(9)
Z	2
ρ_{calc} (g/cm^3)	4.287
μ/mm^{-1}	6.566
F(000)	1376.0
Radiation	MoKα (λ = 0.71073)
2θ range for data collection/°	4.98 to 55.09
Index ranges	$-12 \le h \le 12$, $-12 \le k \le 12$, $-19 \le l \le 19$
Reflections collected	11097
Independent reflections	1012 [R_{int} = 0.0374, R_{sigma} = 0.0189]
Data/restraints/parameters	1012/1/78
Goodness–of–fit on F^2	1.166
Final R indexes [I>=2σ (I)]	R1 = 0.0163, wR2 = 0.0376
Final R indexes [all data]	R1 = 0.0163, wR2 = 0.0377
Largest diff. peak/hole (e Å^{-3})	0.64/–0.47
Flack parameter	0.07(2)

$^a R1 = ||F_o| - |F_c||/|F_o|$; $^b wR2 = [w(F_o^2 - F_c^2)^2]/[w(F_o^2)^2]^{1/2}$.

Table S2. Atomic coordinates (× 10^4), equivalent isotropic displacement parameters ($U_{eq}{}^{a}$, Å^2 × 10^3), and bond valence sums for $K_3Ba_2Zr_6F_{31}$.

atom	Wyckoff site	*x*	*y*	*z*	$U_{eq}{}^{a}$/Å^2	*bond valence sums*
Ba(1)	4*b*	3333.33	6666.67	7444.7(4)	10.19(15)	2.11
Zr(1)	6*c*	2309.3(6)	2309.3(6)	3659.1(4)	6.17(16)	4.09
Zr(2)	6*c*	2556.3(6)	2556.3(6)	6426.0(4)	5.42(16)	4.06
K(1)	6*c*	4287.8(14)	0	5058.0(4)	17.7(3)	0.92
F(1)	12*d*	3112(3)	1573(4)	2556(2)	11.1(6)	1.07
F(2)	2*a*	0	0	3092(5)	13.6(14)	0.79
F(3)	12*d*	3093(4)	4671(4)	3859.6(19)	22.1(8)	1.00
F(4)	6*c*	1975(4)	0	4084(3)	14.7(8)	1.07
F(5)	6*c*	2388(4)	2388(4)	5024(3)	14.3(8)	1.01
F(6)	6*c*	1565(5)	0	6205(2)	13.2(8)	0.99
F(7)	12*d*	2557(4)	4574(4)	6012.6(19)	16.4(7)	1.11
F(8)	6*c*	4531(5)	4531(5)	7064(3)	17.3(9)	0.90

$^{a}U_{eq}$ is defined as one third of the trace of the orthogonalized U_{ij} tensor.

Table S3. Important bond lengths (Å) for $K_3Ba_2Zr_6F_{31}$.

Bond	**Dist./Å**	**Bond**	**Dist./Å**
Ba(1)–F(1)	2.912(3) × 3	Zr(2)–F(1)	2.169(3) × 2
Ba(1)–F(3)	2.807(3) × 3	Zr(2)–F(5)	2.155(5)
Ba(1)–F(7)	2.795(3) × 3	Zr(2)–F(6)	2.1352(10) × 2
Ba(1)–F(8)	2.8228(11) × 3	Zr(2)–F(7)	2.008(3) × 2
Zr(1)–F(1)	2.108(3) × 2	Zr(2)–F(8)	2.106(4)
Zr(1)–F(2)	2.348(3)	K(1)–F(3)	3.314 (4) × 2
Zr(1)–F(3)	1.991(3) × 2	K(1)–F(3)	2.834(4) × 2
Zr(1)–F(4)	2.143(2) × 2	K(1)–F(4)	2.647 (5)
Zr(1)–F(5)	2.094(5)	K(1)–F(5)	3.140 (4)
K(1)–F(6)	3.114 (5)	K(1)–F(7)	2.718 (3) × 2
K(1)–F(7)	2.995 (3)	K(1)–F(8)	3.270 (5)

Table S4. Polymeric Zr–F clusters, linkage modes, and dimensions of Zr-based fluorides.

Compound	Cluster	Linkage modes	Dimension	Reference
$K_3Ba_2Zr_6F_{31}$	$[Zr_6F_{34}]^{10-}$	vertex, edge	1D	This work
$AE_5Zr_3F_{22}$ (AE = Ca, Sr)	$[Zr_8F_{56}]^{24-}$	edge	1D	8, 9
$Rb_5Zr_4F_{21}$	$[Zr_{10}F_{57}]^{17-}$	vertex, edge	1D	10
$A_7Zr_6F_{31}$ (A = Ag, Na)	$[Zr_6F_{36}]^{12-}$	edge	1D	11, 12
$ABaZr_2F_{11}$ (A = Li, Na)	$[Zr_8F_{52}]^{20-}$ $[Zr_4F_{24}]^{8-}$	vertex, edge vertex	1D	13, 14
MZr_2F_{11} (M = La, Pr)	$[Zr_6F_{36}]^{12-}$	edge	1D	15, 16
$M'Zr_3F_{15}$ (M' = La, Lu, Pr, Tl, Y, Yb)	$[Zr_6F_{36}]^{12-}$	edge	3D	16-18
$AgM_3Zr_3F_{20}$ (M = Cd, Hg, Ca)	$[Zr_3F_{18}]^{6-}$	edge	0D	19
$BaZr_2F_{10}$	$[Zr_6F_{38}]^{14-}$	vertex, edge	1D	20

Table S5. Summary of fluorides with 31 F elements in the formula.

Compound	**Space group**	**Symmetry**	**Coordination geometry**	**Dimension**	**Ref.**
$Na_7Zr_6F_{31}$	$R\bar{3}$	CS	ZrF_8	3D	12
$Ag_7Zr_6F_{31}$	$R\bar{3}$	CS	ZrF_8	3D	12
$Na_7M_6F_{31}$	$R\bar{3}$	CS	MF_9	3D	21
$K_7A_6F_{31}$	$R\bar{3}$	CS	AF_9	3D	22, 23
Tl_7BF_{31}	$R\bar{3}$	CS	BF_9	3D	24
$[NH_4]_7C_6F_{31}$	$R\bar{3}$	CS	BF_9	3D	25, 26
$K_5Cr_{10}F_{31}$	$C2/m$	CS	CrF_6, CrF_7	3D	27
$K_3Ba_2Zr_6F_{31}$	$P6_3mc$	NCS	ZrF_8	1D	This work

M = Ce, Tb; A = Th, U, Tb; B = U, Np, Pu; C = U, Pu

Note: CS-centrosymmetric; NCS-noncentrosymmetric

Table S6. Summary of fluorine-rich fluorides (F > 30).

Compound	Space group	Symmetry	Ref.
$Na_3MU_6F_{30}$	$P\bar{3}c1$	CS	28
$Ba_{20}Al_{12}F_{76}$	$I4/m$	CS	29
$Yb_{14}F_{33}$	$R\bar{3}$	CS	30
$Yb_{27}F_{64}$	$R\bar{3}$	CS	31
$(XeF_5)_3(Ti_4F_{19})$	$P2_1/c$	CS	32
$(Xe_2F_3)(Ti_8F_{33})$	$P2/c$	CS	33
$(XeF)_2(Ti_9F_{38})$	Cc	NCS	33
ASc_7F_{30}	$P4_2/n$	CS	34
$Tl_7Pu_6F_{31}$	$R\bar{3}$	CS	24
$Zr_{10}Pb_{19}F_{78}$	$Pmmn$	CS	35
$[NH_4]_7C_6F_{31}$	$R\bar{3}$	CS	25, 26
$[NH_4]_4Ta_6NiF_{36}$	$R\bar{3}c$	CS	36
$Na_2Sr_6ZnFe_6F_{34}$	$C2/c$	CS	37
$Na_7Sr_2Fe_7F_{32}$	$Fddd$	CS	38
$Ca_{14}Y_5F_{43}$	$R\bar{3}$	CS	39
$NaLiBa_7Fe_6F_{34}$	$C2/m$	CS	40
$Ba_7CuFe_6F_{34}$	$C2/m$	CS	41
$Ba_6Cu_{11}F_{34}$	$P\bar{1}$	CS	42
$Ba_{10}Cu_{12}CrF_{47}$	$C2/m$	CS	43
$K_4Ti_8F_{36}\cdot 8HF$	$P\bar{1}$	CS	44
$Rb_4Ti_8F_{36}\cdot 6HF$	$P\bar{1}$	CS	44
$Ca_9Yb_5F_{33}$	-	CS	45
$LiK_{10}Zr_6F_{35}\cdot 2H_2O$	$P2_1$	NCS	46
$K_3Ba_2Zr_6F_{31}$	$P6_3mc$	NCS	This work

M = Al, Ga, Tl, V, Cr, Fe; A = Rb, Tl; B = Re, Os; C = U, Pu

Note: CS-centrosymmetric; NCS-noncentrosymmetric

Table S7. The dipole moments of ZrF_8 units in the unit cell of $K_3Ba_2Zr_6F_{31}$.

Dipole moment (D)			
x	***y***	***z***	**Magnitude (Debye)**
2.4205	0.0823	-19.8108	19.9583

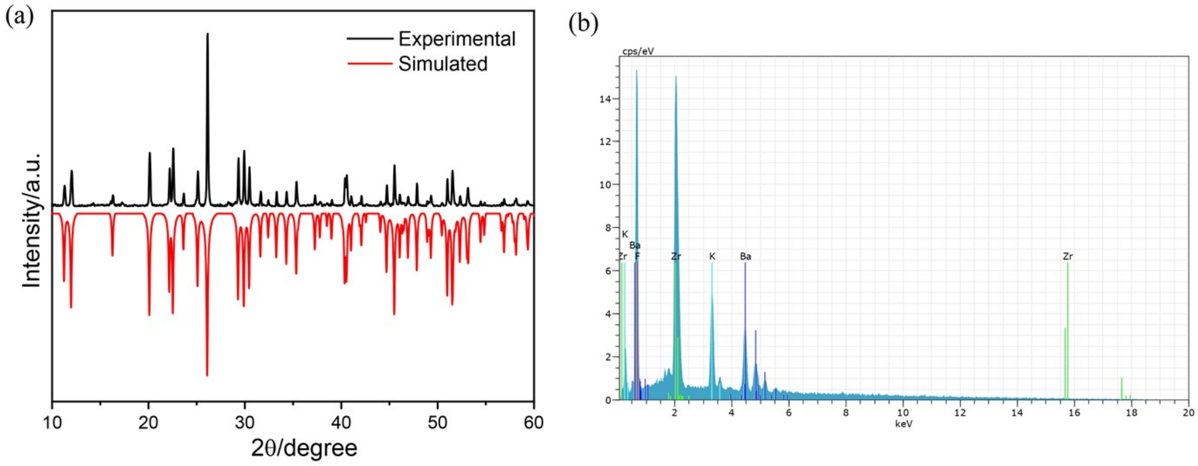

Figure S1. (a) Powder X-ray diffraction pattern and (b) EDS image of $K_3Ba_2Zr_6F_{31}$.

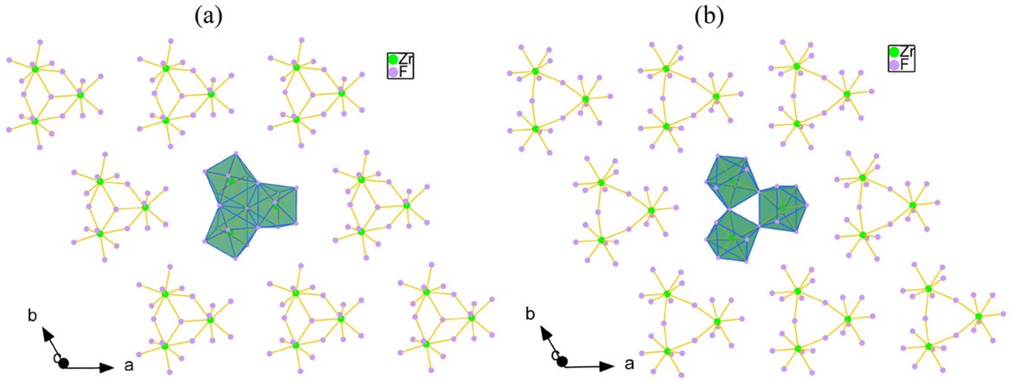

Figure S2. (a) $[Zr(1)_3F_{19}]^{7-}$ clusters made up of edge-sharing $Zr(1)F_8$ units and (b) $[Zr(2)_3F_{21}]^{9-}$ clusters formed by vertex-sharing $Zr(2)F_8$ units.

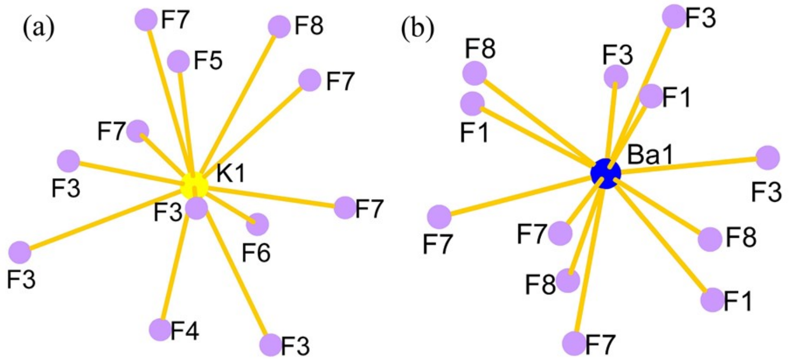

Figure S3. Coordination modes of K(1) and Ba(1) atoms.

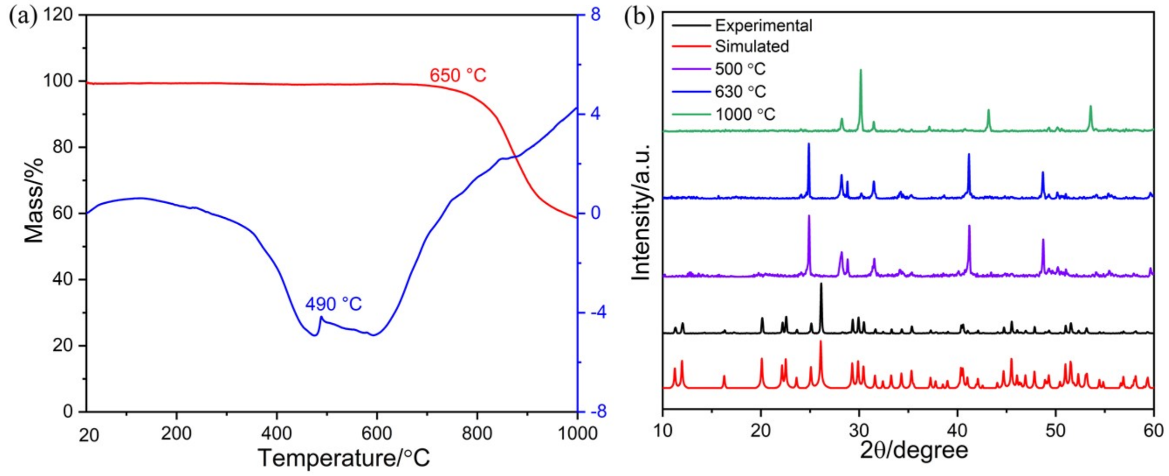

Figure S4. (a) TG curves and (b) XRD patterns of $K_3Ba_2Zr_6F_{31}$ samples heated at different temperatures.

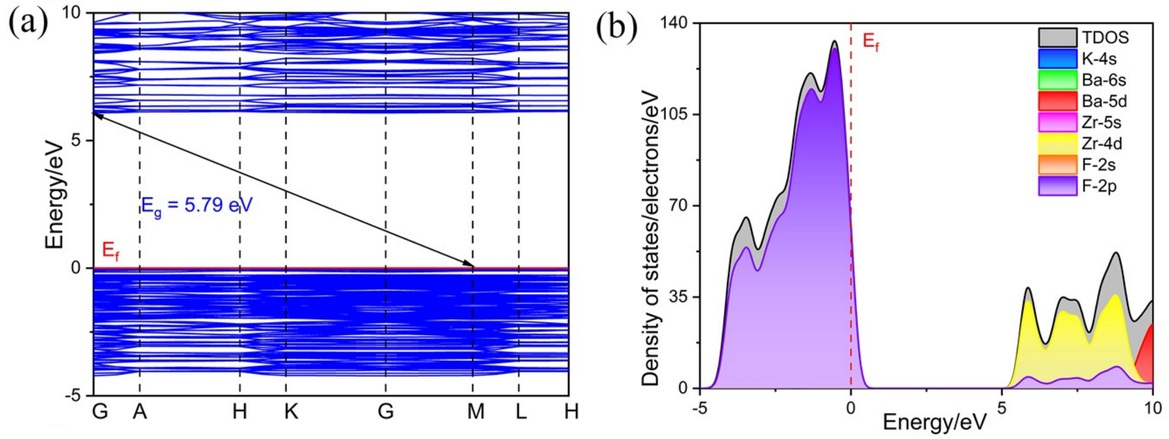

Figure S5. (a) Calculated band structure and (b) density of states (DOS) of $K_3Ba_2Zr_6F_{31}$. The Fermi level is chosen at 0 eV.

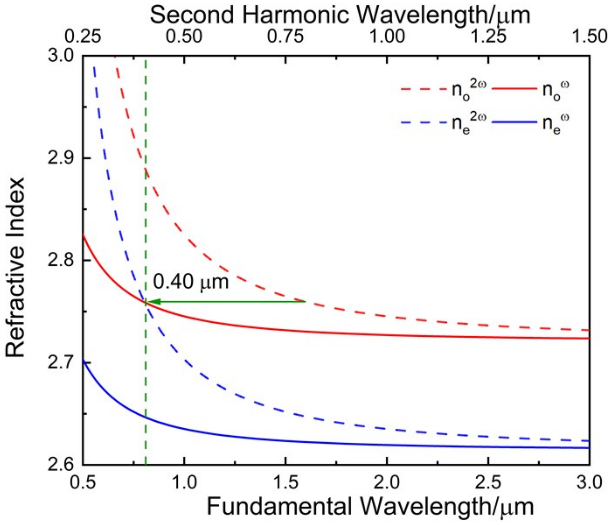

Figure S6. Calculated refractive index dispersion curves and PM range of $K_3Ba_2Zr_6F_{31}$.

References

1. O. V. Dolomanov, L. J. Bourhis, R. J. Gildea, J. A. K. Howard and H. Puschmann, *J. Appl. Crystallogr.*, 2009, **42**, 339–341.

2. S. K. Kurtz and T. T. Perry, *J. Appl. Phys.*, 1968, **39**, 3798–3813.

3. M. D. Segall, P. J. D. Lindan, M. J. Probert, C. J. Pickard, P. J. Hasnip, S. J. Clark and M. C. Payne, *J. Phys.-Condens. Mat.*, 2002, **14**, 2717.

4. J. C. Stewart, D. S. Matthew, J. P. Chris, J. H. Phil, I. J. P. Matt, R. Keith and C. P. Mike, *Z. Kristallogr. - Cryst. Mater.*, 2005, **220**, 567–570.

5. J. Paier, M. Marsman, K. Hummer, G. Kresse, I.C. Gerber and J.G. Ángyán, *J. Chem. Phys.*, 2006, **124**, 154709.

6. W. F. Zhou, W. D. Yao, Q. Zhang, H. G. Xue, S. P. Guo, *Inorg. Chem.*, 2021, **60**, 5198–5205.

7. M. J. Frisch. Gaussian 09, Revision A.02, Gaussian, Inc., Wallingford CT, 2009.

8. A. Oudahmane, M. El-Ghozzi and D. Avignant, *Acta Crystallog. Sect. E*, 2012, **68**, i23.

9. A. Le Bail, *Eur. J. Sol. State Inorg. Chem.*, 1996, **33**, 1211–1222.

10. G. Brunton, *Acta Crystallog. B*, 1971, **27**, 1944–1948.

11. J. H. Burns, R. D. Ellison and H. A. Levy, *Acta Crystallog. B*, 1968, **24**, 230–237.

12. D. Koller and B. G. Müller, *Z. Anorg. Allg. Chem.*, 2000, **626**, 1426–1428.

13. Y. Gao, J. Guery and C. Jacoboni, *ChemInform*, 1993, **24**, 1243–1252.

14. J. P. Laval and A. Abaouz, *J. Solid. State. Chem.*, 1992, **101**, 18–25.

15. C. Martineau, C. Legein, M. Body, O. Péron, B. Boulard and F. Fayon, *J. Solid. State. Chem.*, 2013, 199, 326–333.

16. J. P. Laval and A. Abaouz, *J. Solid. State. Chem.*, 1992, **100**, 90–100.

17. J. Dexpert-ghys, S. J. L. Ribeiro, P. Dugat and D. Avignant, *J. Mater. Chem.*, 1998, **8**, 1043–1050.

18. J. P. Laval, J. F. Gervais, L. Fournès, J. Grannec, P. Gravereau, A. Abaouz and A. Yacoubi, *J. Solid. State. Chem.*, 1995, **118**, 389–396.

19. O. Graudejus and B. G. Müller, *Z. Anorg. Allg. Chem.*, 1996, **622**, 1549–1556.

20. J. P. Laval, B. Frit and J. Lucas, *J. Solid. State. Chem.*, 1988, **72**, 181–192.

21. D. Avignant and J. C. Coussenis, *C. R. Seances Acad. Sci. (Ser. C)*, 1974, 278–613.

22. A. Grzechnik, C. C. Underwood, J. W. Kolis and K. Friese, *J. Fluorine Chem.*, 2013, **150**,

8–13.

23. J. Yeon, M. D. Smith, J. Tapp, A. Möller and H. C. zur Loye, *Inorg. Chem.*, 2014, **53**, 6289–6298.

24. D. Avignant, A. Vedrine and J. C. Coussenis, *C. R. Seances Acad. Sci. (Ser. C)*, 1977, 284–651.

25. P. M. Almond, L. Deakin, A. Mar and T. E. Albrecht-Schmitt, *J. Solid. State. Chem.*, 2001, **158**, 87–93.

26. R. Benz, R. M. Douglass, F. H. Kruse and R. A. Penneman, *Inorg. Chem.*, 1963, **2**, 799–803.

27. Y. Laligant, A. Le Bail, M. Leblanc and G. Ferey, *J. Solid. State. Chem.*, 1990, **85**, 151–158.

28. J. Yeon, M. D. Smith, G. Morrison and H. C. zur Loye, *Inorg. Chem.*, 2015, **54**, 2058–2066.

29. C. Martineau, F. Fayon, M. R. Suchomel, M. Allix, D. Massiot and F. Taulelle, *Inorg. Chem.*, 2011, **50**, 2644–2653.

30. O. Greis, *Z. Anorg. Allg. Chem.*, 1977, **430**, 175–198.

31. N. M. Kompanichenko, A. O. Omel’chuk, O. P. Ivanenko and V. F. Zinchenko, *J. Fluorine Chem.*, 2010, **131**, 282–287.

32. Z. Mazej and E. Goreshnik, *Eur. J. Inorg. Chem.*, 2009, **2009**, 4503–4506.

33. K. Radan, E. Goreshnik and B. Žemva, *Angew. Chem. Int. Ed.*, 2014, **53**, 13715–13719.

34. J. C. Champarnaud-Mesjard and B. Frit, *J. Alloy. Compd.*, 1991, **167**, 319–327.

35 C. Depierrefixe, R. M. Awadallah, J. P. Laval and B. Frit, *Rev. Chim. Miner.*, 1983, **20**, 96–108.

36. R. A. Schöning and G. Meyer, *Z. Anorg. Allg. Chem.*, 1997, **623**, 1759–1762.

37. A. Hemon-Ribaud, M. P. Crosnier-Lopez, J. L. Fourquet and G. Courbion, *J. Fluorine Chem.*, 1994, **68**, 155–163.

38. A. Hemon-Ribaud, J. M. Greneche and G. Courbion, *J. Solid. State. Chem.*, 1994, **112**, 82–91.

39. D. J. M. Bevan, J. Strähle and O. Greis, *J. Solid. State. Chem.*, 1982, **44**, 75–81.

40. A. le Lirzin, J. Soubeyroux, A. Tressaud, R. Georges and J. Darriet, *J. Chim. Phys.*, 1991, **88**, 2173–2189.

41 J. Renaudin, G. Ferey, A. De. Kozak and M. Samouel, *Rev. Chim. Miner.*, 1987, **24**,

295–304.

42. J. Renaudin, J. Pannetier, A. de Kozak, M. Samouël and G. Ferey, *J. Solid. State. Chem.*, 1986, **62**, 164–171.

43. J. Renaudin, G. Ferey, A. De. Kozak and M. Samouel, *Eur. J. Solid State Inorg. Chem.*, 1993, **30**, 401–411.

44. I. M. Shlyapnikov, E. A. Goreshnik and Z. Mazej, *Chem. Commun.*, 2013, **49**, 2703–2705.

45. W. Gettmann and O. Greis, *J. Solid. State. Chem.*, 1978, **26**, 255–263.

46. K. A. Gayvoronskaya, N. A. Didenko, A. B. Slobodyuk, A. V. Gerasimenko and V. Y. Kavun, *J. Fluorine Chem.*, 2011, **132**, 1159–1164.